Proceedings of the 17th World Congress
The International Federation of Automatic Control
Seoul, Korea, July 6-11, 2008

Comparison Studies on Anti-Aliasing/Anti-Imaging Filtering and Signal Extension in Multi-rate ILC

Bin Zhang*, Danwei Wang *,1, Yigang Wang*, Yongqiang Ye*, Keliang Zhou**

* *School of Electrical and Electronic Engineering, Nanyang Technological University, Singapore*
** *Department of Electrical Engineering, Southeast University, Nanjing 210096, China*

Abstract: Multirate iterative learning control (ILC) systems have different sampling rates for feedback online loop and feedforward (or ILC) offline loop. The implementation of multirate ILC requires to downsample the signal first and, after processing, upsample the signal again. In the process of downsampling and upsampling, aliasing and imaging may occur and need to be handled properly. In this paper, the multirate ILC with and without anti-aliasing/anti-imaging filters are compared with different types of low-pass filter. Furthermore, to satisfy the steady state frequency response, the signals are extended and different extension methods are evaluated. A series of simulation results is provided to demonstrate that anti-aliasing and anti-imaging filters significantly improve the tracking performance. However, the extension methods have little influence on the tracking accuracy.

1. INTRODUCTION

For systems that execute repetitively a same tracking operation starting from a same initial condition, iterative learning control (ILC) is a simple and efficient solution to improve tracking accuracy. ILC reaches this goal through adjusting command to a system to compensate its tracking error in previous iteration. There are many forms of learning control, such as D-type ILC based on derivative of error signal, P-type ILC based on tracking error directly, and linear phase lead ILC [4] [2]. Theoretically, with carefully selected parameters, the command provided by ILC, as iteration goes to infinity, will converge to the command that produces the desired output [5].

However, the implementation of ILC subjects to poor learning transient [6]. The error decays initially in a certain number of trials and, after that, it begins to diverge and grows to an unbearable huge value. Simulation shows that after the error grows to a maximum level, it decreases and ultimately reaches a numerical zero [7]. This is consistent with the mathematical convergence proof. The reason of bad learning transient is well explained [6] [7].

There are many works on bad learning transient [6] [7] [8] [9]. The easiest way is to introduce a zero-phase low-pass filer for either tracking error or the command sent to the system [10]. However, the introduction of low-pass filter sacrifices the tracking error and may result in poor tracking accuracy. There is a detailed comparison of different filtering operations on learning performance [5]. Another easy solution is to introduce a linear phase lead in the learning law [4]. However, even with linear phase lead, low-pass filtering is still needed because, in most cases, it is unlikely that linear phase lead can compensate the system phase characteristic into $[90°, -90°]$ on the entire Nyquist frequency range.

Recently, several different forms of multirate ILC schemes are proposed and show promising results to guarantee good learning transient and generate high tracking accuracy simultaneously [11] [12] [13]. Meanwhile, these schemes also demonstrate the abilities to produce good learning behavior with the presence of initial state error, which heavily limits the applications of ILC. Note that the schemes in [12], due to the lost of some high frequency information in downsampling process, cannot reach zero tracking error. However, the cyclic pseudo-downsample ILC scheme [13] can achieve zero tracking error.

In these proposed multirate ILC schemes, the error signal is downsampled to make conditions that guarantee the monotonic decay of tracking error along iteration axis hold. Then, the downsampled signal, whose sampling rate is denoted as *ILC rate*, is upsampled to its original sampling rate, denoted as *feedback rate*. The signal is downsampled by picking one sampling point in a certain number of sampling points given by sampling ratio. In the upsampling, the signal at the *ILC rate* passes through a zero-order-hold to interpolate sampling points between every two points to get its counterpart at the *feedback rate*. In the process of downsamping/upsampling, anti-aliasing and anti-imaging filters need to be applied to prevent the distortion of signal frequency spectra. The application of anti-aliasing/anti-imaging low-pass filter relies on the steady state frequency response concepts. Unfortunately, ILC is a finite time problem and, in a strict

[1] Danwei Wang is with the School of the School of Electrical and Electronic Engineering, Nanyang Technological University, Singapore. edwwang@ntu.edu.sg, Phone:+65-67905376.

sense, the steady state can never be reached. To mitigate this difficulty, the signals are extended at both ends so that the steady state is approximately reached when the signal of interest is filtered.

The purpose of this paper, therefore, seeks to understand and address the effects of anti-aliasing/anti-imaging filtering with different kinds of filter and the effects of different extension methods.

2. PSEUDO-DOWNSAMPLED ILC

For a linear time-invariant system,

$$\begin{cases} x_{f,j}(k+1) = A_f x_{f,j}(k) + B_f u_{f,j}(k) + w_{f,j}(k) \\ y_{f,j}(k) = C_f x_{f,j}(k) + v_{f,j}(k) \end{cases} \quad (1)$$

where the subscript f indicates the *feedback rate*, $k \in [0, p-1]$ with p being the number of total sampling points of a desired trajectory, x is a n dimensional state vector, the input u and the output y are both scalars, subscript j is the cycle index, w and v are the repeated state disturbance and output disturbance, respectively.

An one-step-ahead learning law have the form of:

$$\begin{cases} u_{f,j}(k) = y_d(k) + u_{L,f,j}(k) \\ u_{L,f,j+1}(k) = u_{L,f,j}(k) + \Gamma e_{f,j}(k+1) \end{cases} \quad (2)$$

where Γ is the learning gain, $e_{f,j}(k) = y_d(k) - y_{f,j}(k)$ is the error signal at the j-th cycle with $y_d(k)$ being the desired trajectory. $u_{L,f,j}$ is the adjustment of command in the j-th cycle and $u_{f,j}$ is the input to the closed-loop feedback control system.

The well-known monotonic decay condition, in the frequency domain, is

$$|1 - \Gamma z G(z)| < 1 \quad (3)$$

where $G(z) = C_f(zI - A_f)^{-1}B_f$ is the transfer function of system. Since this condition is generally very difficult to hold for all frequencies up to the Nyquist frequency, a low-pass filter is often introduced at the price of tracking accuracy. In this paper, instead of using a low-pass filter, a multirate ILC scheme is proposed.

The structure of the proposed multirate ILC is illustrated in Figure 1, in which thin line is the closed-loop feedback control system and thick line is the proposed ILC system.

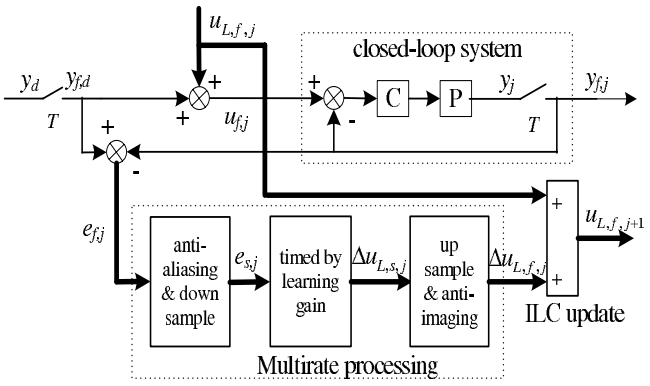

Fig. 1. The scheme of pseudo-downsampled ILC

In this figure, subscript s indicates the slow sampling rate after the downsamling and is denoted as *ILC rate*. C is feedback controller and P is plant. For multirate ILC, error $e_{f,j}$ with sampling period T (*feedback rate*) are downsampled to a rate with a sampling period mT (*ILC rate*), where m is "sampling ratio" [14], and denoted as $e_{s,j}$. Then, this signal times learning gain and is upsampled to *feedback rate* again. The processed signal is shifted one-step-ahead and added to the $u_{L,f,j}$ to accomplish the ILC update law and obtain the $u_{L,f,j+1}$. Clearly, the overall system is a multirate ILC system. The monotonic decay of tracking error is provided in the following Theorem [11].

Theorem 1. For system (1) with repeated disturbances and learning law (6), suppose $|1 - \Gamma C_s B_s| < 1$ with $1 - \Gamma C_s B_s > 0$ and

$$|C_s B_s| \geq \sum_{i=1}^{p_s - 1} \left| C_s A_s^i B_s \right| \quad (4)$$

holds, with $A_s = A_f^m$; $B_s = (A_f^{m-1}B_f + \cdots + A_f B_f + B_f)$; $C_s = C_f$; and p_s the number of sampling points of a given trajectory with respect to the slow rate, then tracking error decay exponentially.

When the signal extension and anti-aliasing/anti-imaging filter are taken into account, the signal flow in the pseudo-downsampled ILC is detailed in Figure 2. First, the tracking error signal $e_{f,j}$ are extended. Then, anti-aliasing filter is applied to prevent the aliasing in downsampling. The filtered signal is truncated to recover its original length. After that, the signal is downsampled and those sampling points that downsampling happens are termed as downsampling points. The downsampled signal at *ILC rate* is timed by learning gain and, then, interpolated by passing through a zero-order-hold to hold the values at downsampling points to recover the signal to *feedback rate*. To prevent the distortion of frequency spectra, this interpellated signal is extended and passes through an anti-imaging filter. Finally, the signal is truncated to recover its original length.

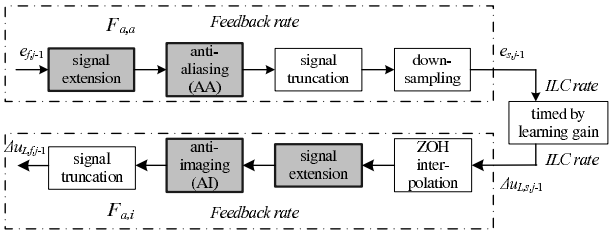

Fig. 2. The signal flow in the multirate ILC

Suppose p_s is trajectory length with respect to slow rate, which is given as

$$p_s = \begin{cases} p/m & p \text{ is multiples of } m \\ \text{int}(p/m) + 1 & \text{otherwise} \end{cases} \quad (5)$$

where $\text{int}(\cdot)$ gets the integer part of (p/m). Then, the ILC update law is summarized as follow:

$$\begin{cases} u_{f,j}(k) = y_{f,d}(k) + u_{L,f,j}(k) \\ u_{L,f,j}(k) = u_{L,f,j-1}(k) + \Delta u_{L,f,j-1}(k+1) \\ \Delta u_{L,f,j-1} = F_{a,i}\left(\Delta u_{L,s,j-1}\right) \\ \Delta u_{L,s,j-1}(i_s) = \Gamma e_{s,j-1}(i_s) \\ e_{s,j-1} = F_{a,a}(e_{f,j-1}) \end{cases} \quad (6)$$

where $F_{a,a}(\cdot)$ and $F_{a,i}(\cdot)$ perform the operations as shown in Figure 2, respectively. where $i_s \in [0, p_s - 1]$ is the index of downsampled signal.

3. THE ANTI-ALIASING FILTERING AND ANTI-IMAGING FILTERING

As shown in Figure 2, the signal needs to be extended before anti-alias filtering and anti-imaging filtering. In this section, some signal extension methods and filtering methods are addressed and their comparison will shown later in simulation.

3.1 Extension Methods

The filtering operation is influenced by the initial condition. As Longman [5] pointed out, the filter response can be considered steady state after roughly one settling time. Therefore, signal extension is sufficient to remove the influence of initial condition on the signal of interest.

Here, three different extension methods are considered and compared.

Method 1: The signal is extended by reflecting through the end-points of the signal. That is, make a mirror reflection of a certain number of sampling points about the end points. The signal with this extension is continuous and has a continuous first order derivative at the end points.

Method 2: The signal is extended by adding zeros. In this case, the signal is no longer continuous.

Method 3: The signal is extended by repeating the end-points of the signal. The signal is continuous but its first order derivative at the end points is no longer continuous.

3.2 The low-pass filter

Different from low-pass filters in traditional ILC aims to cutoff frequency components that do not monotonically decay in learning, the anti-aliasing and anti-imaging filters aim to prevent the frequency spectra distortion in down-sampling and upsampling, respectively.

When downsampling is considered in the frequency domain, m-step downsampling of tracking error signal $e_{f,j}$ will duplicate the spectra of $e_{f,j}$ within $[0, 2\pi/m]$. Therefore, if the bandwidth of $e_{f,j}$ is above frequency $2\pi/m$, the overlapping will definitely occur and the spectra will be distorted. To prevent this phenomenon, an anti-aliasing filter $F_{a,a}$ with a cutoff frequency $2\pi/m$ is required to filter the signal before downsampling.

On the other hand, after the downsampled signal $e_{s,j}$ at *ILC rate* passes through the ILC law, an input update signal $\Delta u_{L,s,j}$ at the *ILC rate* is obtained. This $\Delta u_{L,s,j}$ needs to be upsampled so that it can be added to $u_{L,f,j}$ to achieve the $u_{L,f,j+1}$ at the next iteration. After the upsampling process, the images of the spectra of $u_{L,s,j}$ will appear and, therefore, an anti-imaging filter should be employed to reject those images in frequencies above π/m.

In most cases, a causal filter introduces substantial phase lags. To avoid the additional phase logs, zero-phase low-pass filters are widely used in ILC design. In this paper, three different low-pass filers are selected as anti-aliasing and anti-imaging filters to compare their influences.

Filter 1: An Infinite-duration Impulse Response (IIR) Butterworth Filter

The zero-phase digital filtering can be easily performed by filtering the signal in the forward direction first. After that, the filtered signal sequence is reversed and filtered by the same filter. This way, the resulting signal sequence has precisely zero-phase distortion because the phase lag of the forward direction filtering is canceled by the phase lead of the reverse direction filtering.

Filter 2: A Finite-duration Impulse Response (FIR) Window Filter

For a filter with a given cutoff frequency, its impulse response sequence can be easily obtained from its frequency response. Then, a Hamming window is employed to truncate the infinite impulse response. To realize zero-phase filtering, the filtering point is placed at the middle of the window. The window has a length of $2q + 1$. Obviously, to realize this filter, the signal needs to be extended at end-points.

Filter 3: Cliff filter

A cliff filter tries to achieve a "perfect" cutoff [5]. To realize such a cliff filter, the signal is first transformed into the frequency domain through a discrete Fourier transform. Then, those frequency components reside in frequencies above the cutoff frequency are deleted. This signal is then taken the inverse transform to obtain the filtered signal in the time domain. It is a non-causal filter with zero phase shift.

4. SIMULATION RESULTS

To compare the performance of the ILC scheme with above mentioned extension methods and filters, a system (7) is employed and suppose the sampling frequency (*feedback rate*) is 100Hz. That is, the sampling period is 0.01 second.

$$G_p(s) = \frac{948}{s^2 + 42s + 948} \tag{7}$$

The trajectory is defined as (8), which has a length of 10 seconds and contains two high frequency components at 8Hz and 10Hz, respectively.

$$\begin{aligned} y_d(t) =& 45(1 - \cos(0.2\pi t)) + \\ & 0.15(1 - \cos(16\pi t)) + 0.05(1 - \cos(20\pi t)) \end{aligned} \tag{8}$$

4.1 Parameter selection

Learning gain Γ A high learning gain, although can generate a fast convergence speed, may degrade the tracking performance in steady state response in the sense that random noise going through the learning law will be amplified [15]. Hence, a low value learning gain is suggested.

The learning gain has a range of $0 < \Gamma < 1/C_s B_s$. For (7), when sampling period changes from 0.01 second to 0.1 second (the *sampling ratio* changes from 1 to 10), all the values of $1/C_s B_s$ for these different *sampling ratios* are larger than 1. Therefore, the learning gain Γ is selected conservatively as 0.5.

Sampling ratio m We discretize the system model (7) using the sampling period $T = 0.01$ second. Then, the sign of $1 - \Gamma C_f B_f$ is checked. If condition (4) holds, the sampling rate does not need to be reduced. On the other hand, if the required condition is violated, the sampling period is increased to $2T$, $3T$, and so on. This process is repeated until the required condition holds for a sampling period mT.

The trajectory (8) has 200 sampling points. With $T = 0.01$ second, $|1 - \Gamma C_f B_f| = 0.9795 < 1$ and $1 - \Gamma C_f B_f = 0.9795 > 0$. The left hand side of (4) is 0.0411, while the right hand side of (4) is 1.0717. Clearly, (4) is not satisfied. Increase the sampling period and when it becomes 0.05 second, $|1 - \Gamma C_s B_s| = 0.7226 < 1$ and $1 - \Gamma C_s B_s = 0.7226 > 0$. The first Markov parameter is 0.5548, while the sum of all the remaining Markov parameters' absolute value is 0.5523. Condition (4) is satisfied. Note that when sampling period becomes 0.05 second, the number of sampling points p_s is 200. Finally, m is selected as 5.

Cutoff frequency f_c The sampling theorem states that any signal can be reconstructed from sampling values as long as it is sampled at a rate at least twice the highest frequency present in the signal. Failure to do so results in aliasing meaning that high frequency components will appear in lower frequencies. To avoid the aliasing problem, a low pass filter is applied to remove the frequency components above half the sampling frequency. Suppose the signal is downsampled by a ratio m, the bandwidth should be band limited by π/m. Suppose the Nyquist frequency is F_{ny}, then, the cutoff frequency of anti-aliasing and anti-imaging filter should be set as F_{ny}/m. With Nyquist frequency 50Hz and m=5, the cutoff frequency f_c is given as 10Hz.

4.2 Simulation results

In the following simulations, the Butterworth filter is 5th order, the window of the window filter has a length of 101 points and 100 sampling points are added at both ends of the signal.

A conventional ILC is used to compare with multirate ILC. The conventional ILC has a learning law given in (2) with a zero-phase low-pass filter is used to cut off frequencies beyond the learnable bandwidth.

Figure 3 shows the tracking performance, given by root mean square (RMS) error, of conventional ILC with three different low-pass filters. Note that, the low pass filter here is to cut off high frequencies that cannot make condition (3) hold. The cutoff frequency is 3.5Hz, which is obtained by discretizing the system (7) and then evaluating condition (3). The extension method 3 is used, that is, repeating the end-points of the signal. It can be seen that, although the difference is not obvious, the window filter shows the best tracking performance while the cliff filter shows the worst.

Figure 4 shows the tracking accuracies of conventional ILC with a cutoff frequency of 3.5Hz, multirate ILC without anti-aliasing and anti-imaging filters, and multirate ILC with them. It is clear that multirate ILC has better performance than conventional ILC, while the introduction of

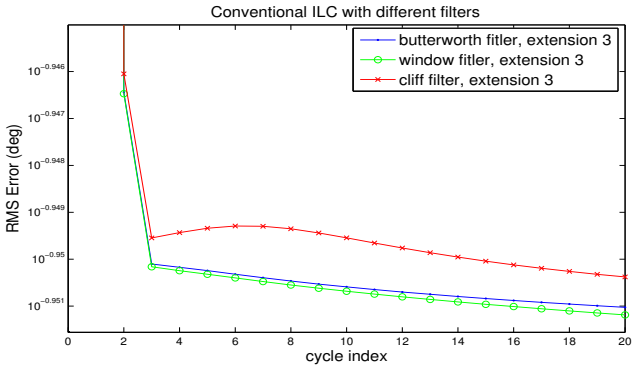

Fig. 3. Conventional ILC

anti-aliasing and anti-imaging filters further improves the tracking accuracy. When filters are used, extension method 3 is used.

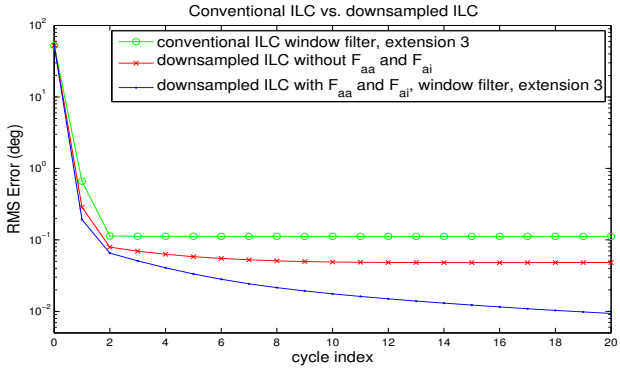

Fig. 4. Comparison among multirate ILC with/without anti-aliasing and anti-imaging filter and conventional ILC

To highlight the advantages of the anti-aliasing and anti-imaging filter, the tracking error signals from these three different learning methods are shown in Figure 5 and the power spectra of these error signals are compared in Figure 6. Note that in Figure 5, the scales of the three subfigures are the same and the improvement of tracking error is remarkable. The tracking error of conventional ILC, downsampled ILC and downsampled ILC with anti-aliasing/anti-imaging filters are 0.25°, 0.15°, and 0.02°, respectively. The power spectra comparison in Figure 6 show that most error components below 10Hz has been removed by the multirate ILC with anti-aliasing and anti-imaging filters. While the other two schemes cannot suppress some error components in these frequencies, which results in large tracking error. The input signals are shown in Figure 7.

Figure 8 shows the multirate ILC with different anti-aliasing and anti-imaging filters. The extension method 3 is used again. The results show that window filter and Butterworth filter have the similar tracking accuracy, which are better than that of cliff filter.

Next, let's investigate the influence of different extension methods. The results are shown in Figures 9, 10, and 11 with Butterworth filter, window filter, and cliff filter, respectively. First of all, these figures show that different

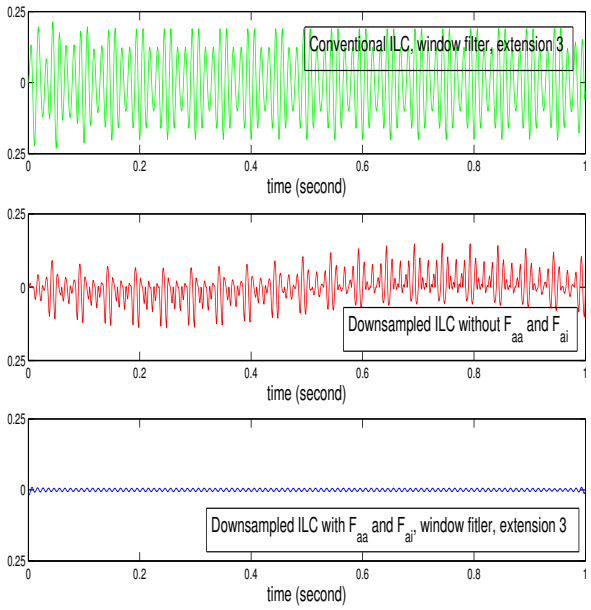

Fig. 5. Comparison of tracking error signal

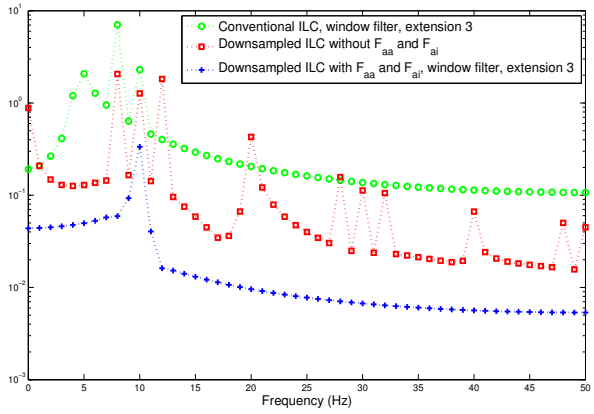

Fig. 6. Comparison of frequency spectra

extension methods only cause very slight difference in tracking accuracy. Second, to get the best tracking accuracy, different filters requires different extension methods. In practice, since the difference on tracking accuracy of these extension methods are so small and neglectable, extension method can be randomly selected.

Note that in traditional multirate signal processing, when a slow rate signal is upsampled, zeros are added between two sampling points rather than using a zero-order-hold. This adding zeros interpolation method is evaluated under different filters and compared with conventional ILC as shown in Figure 12. It is clear from this figure that the tracking accuracy of this interpolation method is much poorer than conventional ILC.

From the results from Figure 3 to 12, some conclusions can be drawn: 1. Multirate ILC has better tracking performance than conventional ILC. 2. Anti-aliasing and anti-imaging filters in multirate ILC further improve the tracking performance. 3. Window filter and Butterworth filter, in most cases, have better tracking than cliff filter. 4. Interpolation through passing a zero-order-holder is necessary. 5. Extension methods have little influence on tracking performance.

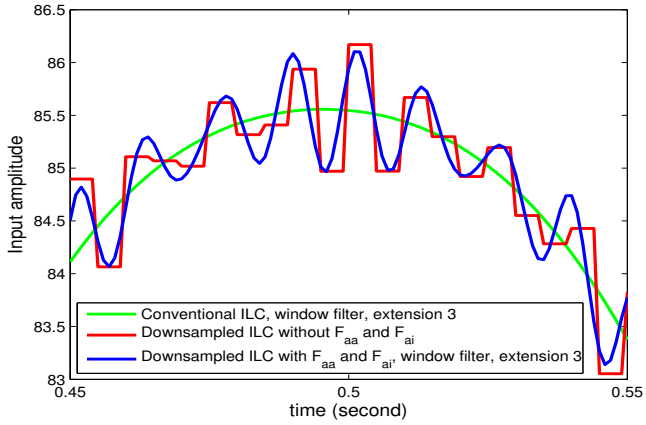

Fig. 7. Comparison of input signal

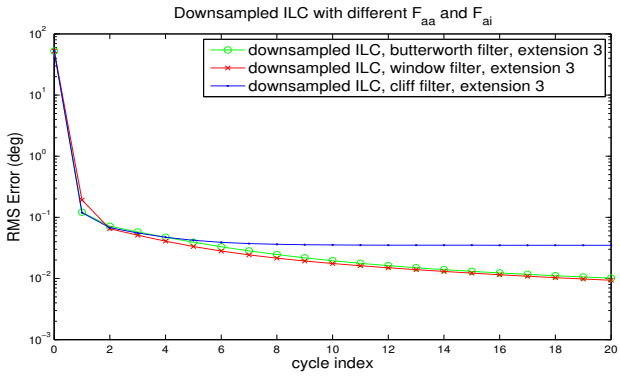

Fig. 8. Multirate ILC with different anti-aliasing and anti-imaging filters

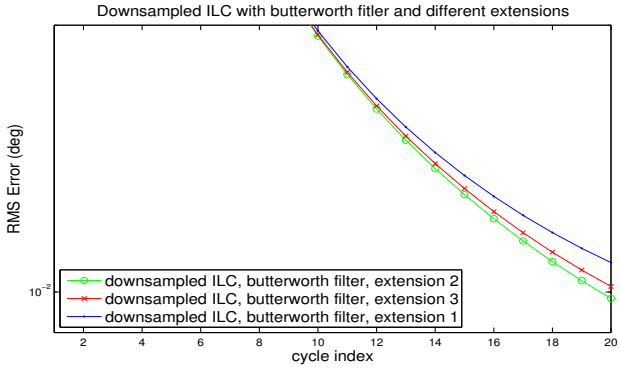

Fig. 9. DownsampledlILCwithButterworthFilter

5. CONCLUSION AND FUTURE WORKS

In this paper, the implementation of a multirate iterative learning control, pseudo-downsampled ILC, is examined. The influence of anti-aliasing and anti-imaging filters on the tracking performance is investigated under three different kinds of low-pass filters, Butterworth filter, window fil-

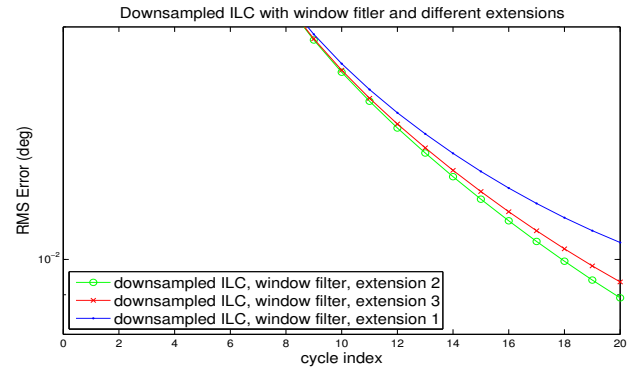

Fig. 10. DownsampledlILCwithWindowFilter

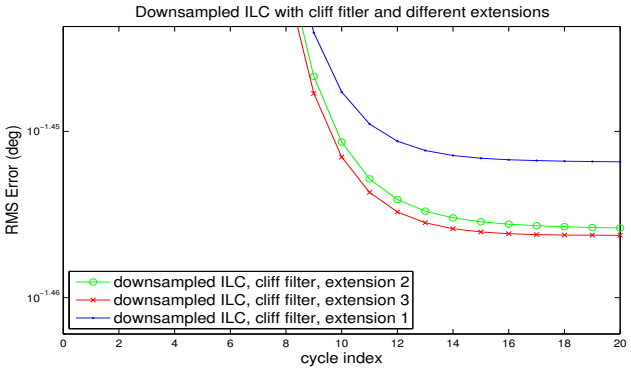

Fig. 11. DownsampledlILCwithCliffFilter

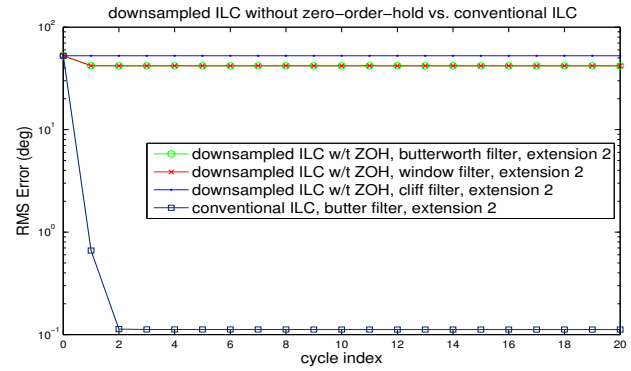

Fig. 12. DownsampledILCwithoutZOH

ter and cliff filter. To realize zero-phase filtering and satisfy the steady state frequency response of filtering, the signals are extended with different methods. The influences of these extension methods on the tracking performance are discussed. Simulation results are presented to evaluate the different combination of different filters and different extension methods and some useful conclusions are drawn.

This paper considers several widely used filters and signal extension methods. In the future, the effects of other filters, including using different windows and window lengths in a window filter will be investigated. Moreover, some experiment verifications will be carried out. To eliminate the phase lag caused by some filters, it is also worth to investigate other zero-phase filters for anti-aliasing and anti-imaging. Finally, some efforts are necessary to analyze the stability and errors associated with the process of resampling and filtering.

REFERENCES

[1] C. J. Chien and J. S. Liu, "A P-type iterative learning controller for robust output tracking of nonlinear time-varying systems," *Intl. Journal of Control*, vol. 64, pp. 319–334, 1996.

[2] B. Zhang, D. Wang, and Y. Ye, "Wavelet transform based frequency tuning ILC," *IEEE Trans. on System, Man, and Cybernetics, Part B*, vol. 35, pp. 107–114, Feb. 2005.

[3] Y. Wang and R. W. Longman, "Use of non-causal digital signal processing in learning and repetitive control," *Advances in the Astronautical Sciences*, vol. 90, pp. 649–668, 1996.

[4] D. Wang, "On D-type and P-type ILC designs and anticipatory approach," *International Journal of Control*, vol. 73, pp. 890–901, 2000.

[5] A. M. Plotnik and R. W. Longman, "Subtleties in the use of zero-phase low-pass filtering and cliff filtering in learning control," *Advances in the Astronautical Sciences*, vol. 103, pp. 673–692, 1999.

[6] C.-K. Chang, R. W. Longman, and M. Q. Phan, "Techniques for improving transients in learning control systems," *Advances in Astronautical Sci.*, vol. 76, pp. 2035–2052, 1992.

[7] R. W. Longman, "Iterative learning control and repetitive control for engineering practice," *Intl. Journal of Control*, vol. 73, no. 10, pp. 930–954, 2000.

[8] Y.-Q. Chen and K. L. Moore, "Frequency domain adaptive learning feedforward control," in *IEEE Symp. on Comput. Intell. in Robot. and Automat.*, (Canada), pp. 396–401, 2001.

[9] D.-N. Zheng and A. Alleyne, "An experimental study for an iterative learning control scheme with adaptive filtering," in *2002 ASME Int. Mechanical Engineering Congress and Exposition*, (LA USA), pp. 1–9, 2002.

[10] E. J. Solcz and R. W. Longman, "Disturbance rejection in repetitive controller," *Advances in the Astronautical Sciences*, vol. 76, pp. 2111–2130, 1992.

[11] B. Zhang, D. Wang, Y. Ye, Y. Wang, and K. Zhou, "Two-mode ILC with pseudo-downsampled learning in high frequency range," *International Journal of Control*, vol. 80, pp. 349–362, . 2007.

[12] B. Zhang, D. Wang, Y. Ye, Y. Wang, and K. Zhou, "Pseudo-downsampled iterative learning control," *Intl. J. Robust and Nonlinear Control*, in print.

[13] B. Zhang, D. Wang, Y. Ye, Y. Wang, and K. Zhou, "Experimental study on pseudodownsampled ilc with time shift along iteration axis," in *Proc. of American Control Conf.*, (MN. USA), pp. 244–249, June 2006.

[14] N. Sadegh, A. Hu, and C. James, "Synthesis, stability analysis, and experimental implementation of a multirate repetitive learning controller," *Trans. of ASME: J. of Dynamic Systems, Measurement, and Control*, vol. 124, pp. 668–674, Dec. 2002.

[15] R. W. Longman and S.-L. Wirkander, "Automated tuning concepts for iterative learning and repetitive control laws," in *Proc. 37th CDC*, (FL. USA), pp. 192–198, 1998.